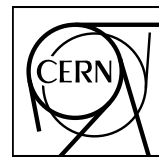


EUROPEAN ORGANIZATION FOR NUCLEAR RESEARCH



ALICE



CERN-PH-EP-2013-132

July 18, 2013

 K_S^0 and Λ production in Pb–Pb collisions at $\sqrt{s_{NN}} = 2.76$ TeV

ALICE Collaboration*

Abstract

The ALICE measurement of K_S^0 and Λ production at mid-rapidity in Pb–Pb collisions at $\sqrt{s_{NN}} = 2.76$ TeV is presented. The transverse momentum (p_T) spectra are shown for several collision centrality intervals and in the p_T range from 0.4 GeV/c (0.6 GeV/c for Λ) to 12 GeV/c. The p_T dependence of the Λ/K_S^0 ratios exhibits maxima in the vicinity of 3 GeV/c, and the positions of the maxima shift towards higher p_T with increasing collision centrality. The magnitude of these maxima increases by almost a factor of three between most peripheral and most central Pb–Pb collisions. This baryon excess at intermediate p_T is not observed in pp interactions at $\sqrt{s} = 0.9$ TeV and at $\sqrt{s} = 7$ TeV. Qualitatively, the baryon enhancement in heavy-ion collisions is expected from radial flow. However, the measured p_T spectra above 2 GeV/c progressively decouple from hydrodynamical-model calculations. For higher values of p_T , models that incorporate the influence of the medium on the fragmentation and hadronization processes describe qualitatively the p_T dependence of the Λ/K_S^0 ratio.

*See Appendix A for the list of collaboration members

Collisions of heavy nuclei at ultra-relativistic energies are used to investigate a deconfined high temperature and density state of nuclear matter, the quark–gluon plasma. The transverse momentum (p_T) spectra of identified hadrons and their ratios provide a means for studying the properties of this state of matter and the mechanisms that transform quasi-free partons into observed hadrons. It was observed at the Relativistic Heavy Ion Collider (RHIC) [1, 2], that the Λ/K_S^0 and p/π ratios at intermediate p_T (from about 2 to about 6 GeV/c) are markedly enhanced in central heavy-ion collisions when compared with the peripheral or pp results. A similar observation was also made at the Super Proton Synchrotron [3]. These observations led to a revival and further development of models based on the premise that deconfinement opens an additional mechanism for hadronization by allowing two or three soft quarks from the bulk to combine forming a meson or a baryon [4, 5]. The baryons then appear at a higher p_T than the mesons, since their momentum is the sum of the momenta of three quarks, instead of only two. If the (anti-)quarks generated by (mini)jet fragmentation are also involved in recombination [6], the baryon enhancement could extend to even higher momenta, up to 10–20 GeV/c [7]. At lower p_T , the hydrodynamical radial flow also contributes to the baryon enhancement, because the baryons, being heavier, are pushed to higher p_T than the mesons. But the applicability of such models is limited to transverse momenta below 2 GeV/c, above which the observed p_T spectra start to deviate from hydrodynamical calculations.

The evolution of the baryon to meson ratio with collision energy, comparisons with pp events and a study of the centrality dependence in nucleus–nucleus collisions provides additional information about this “baryon anomaly” [8]. In Pb–Pb collisions at the Large Hadron Collider (LHC) energies, that are around 14 times higher than those at RHIC, the maximum of the Λ/K_S^0 ratio is expected to be shifted towards higher p_T , because of an increased partonic radial flow [4, 5]. In contrast, the Λ/K_S^0 ratio measured in elementary pp collisions should not change significantly with the center-of-mass energy, since the particle production is presumably dominated by fragmentation processes.

The relative contribution of different hadronization mechanisms changes with hadron momentum. While at intermediate p_T recombination might be dominating, fragmentation could take over at higher p_T , depending on the underlying momentum distributions of the quarks. For this reason it is important to identify baryons and mesons in a wide momentum range. The topological decay reconstruction of K_S⁰ and Λ provides an opportunity to extend the baryon and meson identification from low to high transverse momenta, which can not easily be achieved using other particle identification methods without introducing additional systematic effects.

In this Letter we present the K_S⁰ and Λ transverse-momentum spectra and the Λ/K_S^0 ratios from Pb–Pb collisions at $\sqrt{s_{NN}} = 2.76$ TeV recorded in November 2010’s heavy-ion run of the LHC. The p_T dependence of the Λ/K_S^0 ratios is compared with pp results obtained at $\sqrt{s} = 0.9$ and 7 TeV, that bracket the Pb–Pb measurements in energy.

A description of the ALICE apparatus can be found in [9]. For the analysis presented here, we used the Time Projection Chamber (TPC) and the Inner Tracking System (ITS) to reconstruct charged particle tracks within the pseudo-rapidity interval of $|\eta| < 0.9$. Particle momenta were determined from the track curvature in a magnetic field of 0.5 T. The two VZERO scintillator counters, covering pseudo-rapidity ranges of $2.8 < \eta < 5.1$ (VZERO-A) and $-3.7 < \eta < -1.7$ (VZERO-C), provided a signal proportional to the number of charged particles in these acceptance regions. The VZERO detectors together with the two innermost Silicon Pixel Detector (SPD) layers of the ITS, positioned at radii of 3.9 and 7.6 cm (acceptance $|\eta| < 2.0$ and $|\eta| < 1.4$ respectively), were used as an interaction trigger. To select a pure sample of hadronic interactions, only events with at least one particle hit in each of the three trigger detectors (SPD, VZERO-A and VZERO-C) were accepted offline. The selected events were required to have reconstructed primary vertices with a position along the beam direction within ± 10 cm of the nominal center of the detector to ensure a uniform acceptance in pseudo-rapidity for the particles under study. The events were then classified according to the collision centrality, based on the

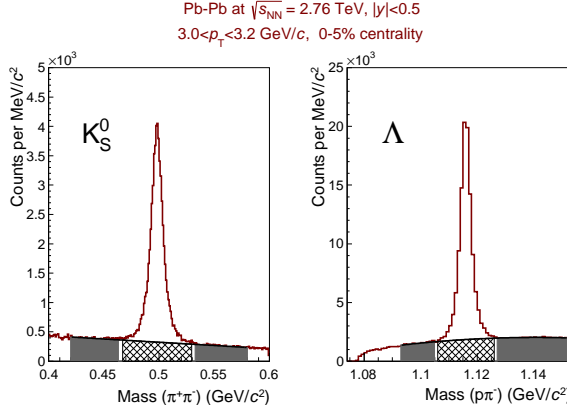


Fig. 1: Examples of invariant mass distributions for K_S^0 and Λ . The filled areas to the sides of the peaks were used to fit the background in order to estimate the background level under the peaks, indicated as the light shaded areas.

sum of the amplitudes in the VZERO counters fitted with a Glauber model description of the collisions, as discussed in [10]. After these selections, we retained for the final analysis 13 million events in the collision centrality range from 0 to 90% of the nuclear cross-section.

The weakly decaying neutral hadrons (K_S^0 and Λ) were reconstructed using their distinctive V-shaped decay topology in the channels (and branching ratios) $K_S^0 \rightarrow \pi^+\pi^-$ (69.2%) and $\Lambda \rightarrow p\pi^-$ (63.9%) [11]. The reconstruction method forms so-called V0 decay candidates and the details are described in [12]. Because of the large combinatorial background in Pb–Pb collisions, a number of topological selections had to be more restrictive than those used in the pp analysis. In particular, the cuts on the minimum distance of closest approach between the V0 decay products and on the minimum cosine of the V0 pointing angle (the angle between the line connecting the primary and V0 vertices and the V0 momentum vector) [12] were changed to one standard deviation and to 0.998, respectively. In addition, we retained only the V0 candidates reconstructed in a rapidity window of $|y| < 0.5$, with their decay-product tracks within the acceptance window $|\eta| < 0.8$. To further suppress the background, we kept only V0 candidates satisfying the cut on the proper decay length $l_T \cdot m / p_T < 3 c\tau$ ($4 c\tau$), where l_T and m are the V0 transverse decay length and nominal Λ (K_S^0) mass [11], and $c\tau$ is 7.89 cm (2.68 cm) for Λ (K_S^0) [11]. For the Λ candidates with $p_T < 1.2 \text{ GeV}/c$, a conservative three-standard-deviation particle-identification cut on the difference between the specific energy loss (dE/dx) measured in the TPC and the expected energy loss as defined by a momentum-dependent parameterization of the Bethe–Bloch curve was applied for the proton decay-product tracks. To reduce the contamination of Λ reconstructed as K_S^0 , an additional selection was applied in the Armenteros–Podolanski variables [13] of K_S^0 candidates, rejecting candidates with $p_T^{\text{arm}} < 0.2 \times |\alpha^{\text{arm}}|$. Here, p_T^{arm} is the projection of the positively (or negatively) charged decay-product momentum on the plane perpendicular to the V0 momentum. The decay asymmetry parameter α^{arm} is defined as $\alpha^{\text{arm}} = (p_{||}^+ - p_{||}^-)/(p_{||}^+ + p_{||}^-)$, where $p_{||}^+$ ($p_{||}^-$) is the projection of the positively (negatively) charged decay-product momentum on the momentum of the V0. The minimal radius of the fiducial volume of the secondary vertex reconstruction was chosen to be 5 cm to minimize systematic effects introduced by efficiency corrections. It was verified that the decay-length distributions reconstructed within this volume were exponential and agreed with the $c\tau$ values given in the literature [11].

The raw yield in each p_T bin was extracted from the invariant-mass distribution obtained for this momentum bin. Examples of such distributions are shown in Fig. 1. The raw yield was calculated by subtracting a fit to the background from the total number of V0 candidates in the peak region. This region was $\pm 5\sigma$ for K_S^0 , and $\pm(3.5\sigma + 2 \text{ MeV}/c^2)$ (to better account for tails in the mass distribution at low p_T) for Λ . The σ was obtained by a Gaussian fit to the mass peaks. The background was determined by fitting polynomials of first or second order to side-band regions left and right of the peak region.

The overall reconstruction efficiency corrections were extracted from a procedure based on HIJING events [14] and using GEANT3 [15] for transporting simulated particles, followed by a full calculation of the detector responses and reconstruction done with the ALICE simulation and reconstruction framework [16]. The estimated efficiency included the geometrical acceptance of the detectors, track reconstruction efficiency, the efficiency of the applied topological selection cuts, and the branching ratios for the V0 decays. The typical efficiencies for both particles were about 30% for $p_T > 4 \text{ GeV}/c$, dropping to 0 at $p_T \sim 0.3 \text{ GeV}/c$. The efficiencies did not change with the event centrality for p_T above a few GeV/c . However, at lower p_T , they were found to be dependent on the event centrality. For Λ at $p_T < 0.9 \text{ GeV}/c$ the difference is about factor 2 between the 0–5% and 80–90% centrality intervals. This was because the distributions of the topological variables used in the selections were changing with the centrality, whereas the corresponding threshold cut values were kept constant. The effect was well reproduced by the Monte Carlo simulations. The final momentum spectra were therefore corrected in each centrality bin separately.

The spectra of Λ were in addition corrected for the feed-down contribution coming from the weak decays of Ξ^- and Ξ^0 . For this purpose, a two-dimensional response matrix, correlating the p_T of the detected decay Λ with the p_T of the decayed Ξ , was generated from Monte-Carlo simulations. By normalizing this matrix to the measured Ξ^- spectra [17], the distributions of the feed-down Λ were determined and subtracted from the inclusive Λ spectra. The phase space distribution and total yield for the Ξ^0 were assumed to be the same as for the Ξ^- . The feed-down correction thus obtained was found to be a smooth function of p_T with a maximum of about 23% at $p_T \sim 1 \text{ GeV}/c$ and monotonically decreasing to 0% at $p_T > 12 \text{ GeV}/c$. As a function of centrality, this correction changed by only a few per cent.

Since the ratio Ξ^-/Ω^- in Pb–Pb collisions at $\sqrt{s_{\text{NN}}} = 2.76 \text{ TeV}$ was measured to be about 6 [18], and taking into account that the branching ratio $\Omega^- \rightarrow \Lambda K^-$ is 67.8% [11], the feed-down contribution from decays of Ω^- baryons would be about 1%, which is negligible compared with other sources of uncertainty (see below). Also, we did not correct the Λ spectra for the feed-down from non-weak decays of Σ^0 and $\Sigma(1385)$ family.

The fraction of Λ 's produced in hadronic interactions with the detector material was estimated using the detailed Monte Carlo simulations mentioned above. Since this fraction was found to be less than 1%, it was neglected.

The following main sources of systematic uncertainty were considered: raw yield extraction, feed-down, efficiency corrections, and the uncertainty on the amount of crossed material. These were added in quadrature to yield the overall systematic uncertainty on the p_T spectra for all centralities.

The systematic uncertainties on the raw yields were estimated by using different functional shapes for the background and by varying the fitting range. Over the considered momentum range, the obtained raw yields varied within 3% for K_S⁰ and 4–7% for Λ .

As a measure for the systematic uncertainty of the feed-down correction, we used the spread of the values determined for different centrality ranges with respect to the feed-down correction estimated for minimum bias events. This deviation was found to be about 5% relative to the overall Λ yield.

The systematic uncertainty associated with the efficiency correction was evaluated by varying one-by-one the topological, track-selection and PID cuts. The cut variations were chosen such that the extracted uncorrected yield of the K_S⁰ and Λ would change by 10%. To measure the systematic uncertainty related to each cut, we used as a reference the corrected spectrum obtained with the nominal cut values. For Λ , the feed-down correction was re-evaluated and taken into account for every variation of the cut on the cosine of the pointing angle. The overall p_T -dependent systematic uncertainty associated with the efficiency correction was then estimated by choosing the maximal (over all cut variations) deviation between varied and nominal spectra values obtained in each momentum bin. For the momentum range

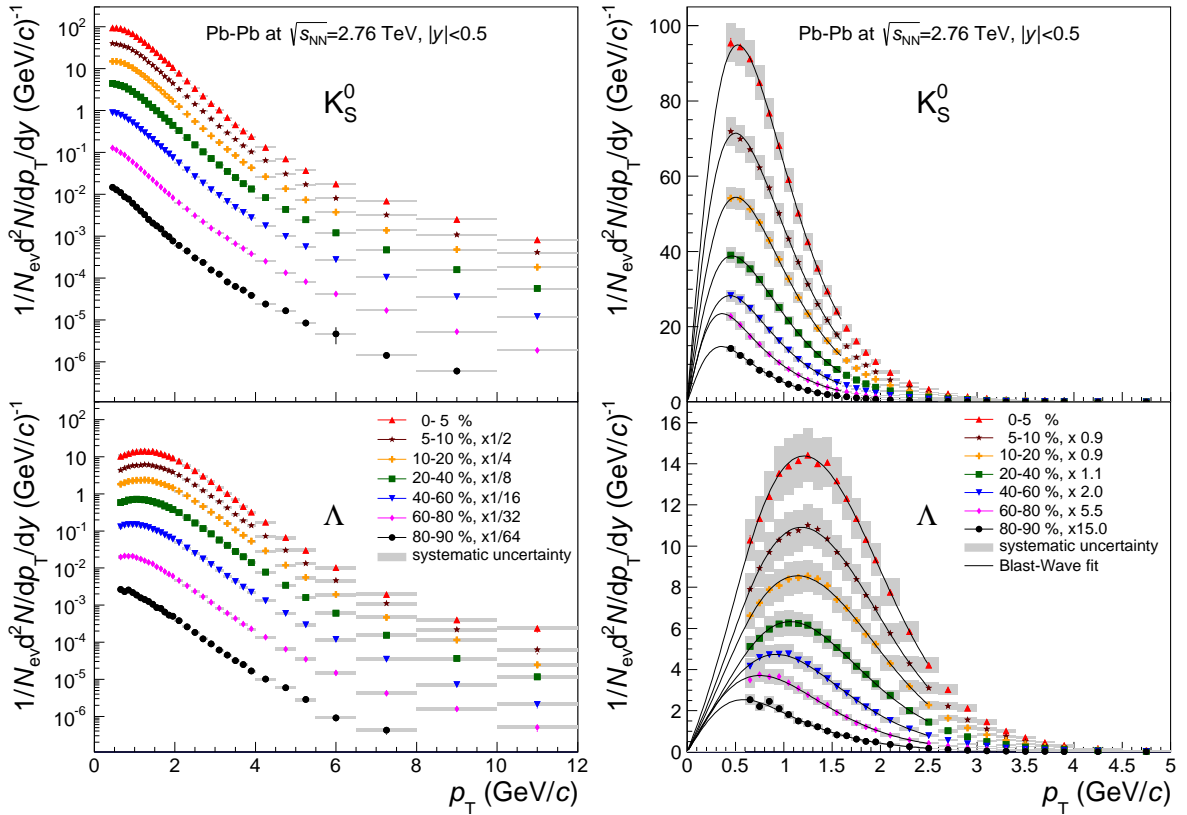


Fig. 2: K_S^0 and Λ transverse momentum spectra for different event centrality intervals shown in logarithmic (left) and linear (right) scale. The curves represent results of blast-wave fits [19].

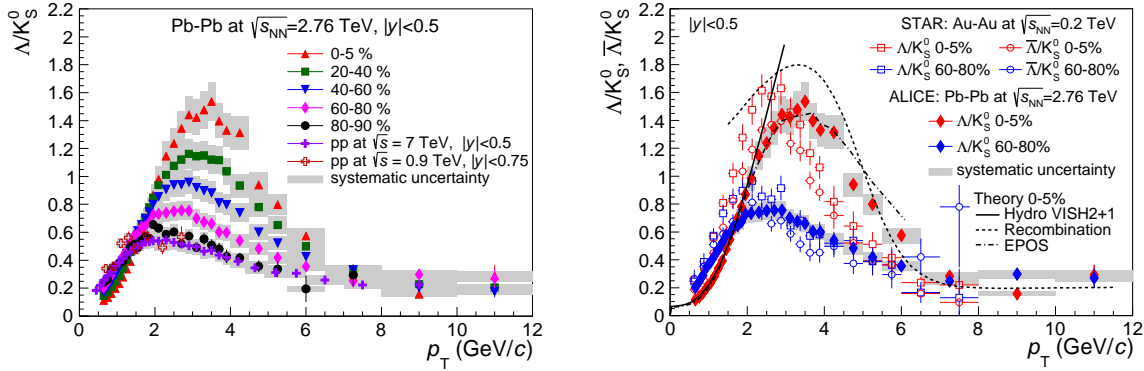


Fig. 3: Left: Λ/K_S^0 ratios as a function of p_T for different event centrality intervals in Pb–Pb collisions at $\sqrt{s_{NN}} = 2.76$ TeV and pp collisions at $\sqrt{s} = 0.9$ [12] and 7 TeV [20]. Right: Selected Λ/K_S^0 ratios as a function of p_T compared with Λ/K_S^0 and $\bar{\Lambda}/K_S^0$ ratios measured in Au–Au collisions at $\sqrt{s_{NN}} = 200$ GeV [21]. The solid, dashed and dot-dashed lines show the corresponding ratios from a hydrodynamical model [22, 23, 24], a recombination model [25] and the EPOS model [26], respectively.

considered, this systematic uncertainty was determined to be 4–6% for both K_S^0 and Λ .

The systematic uncertainty introduced because of possible imperfection in the description of detector material in the simulations was estimated in [12] and amounted to 1.1–1.5% for K_S^0 and 1.6–3.4% for Λ .

Since the systematic uncertainties related to the efficiency correction are correlated for the Λ and K_S^0 spectra, they partially cancel in the Λ/K_S^0 ratios. These uncertainties were evaluated by dividing Λ and K_S^0 spectra obtained with the same cut variations and found to be half the size of those that would be obtained if the uncertainties of the Λ and K_S^0 spectra were assumed to be uncorrelated. Altogether, over the considered momentum range, the maximal systematic uncertainty for the measured Λ/K_S^0 ratios was found to be about 10%.

The transverse-momentum spectra of K_S^0 obtained in different centrality intervals were compared with the spectra of charged kaons also measured by ALICE [27]. The two sets of spectra agree within the systematic uncertainties.

The corrected p_T spectra are shown in logarithmic scale in Fig. 2 (left). The spectra were fitted using the blast-wave parameterization described in [19]. The resulting curves are superimposed in Fig. 2 (right), with a linear scale and for a restricted momentum range, to emphasize the low- p_T region. The fit range in p_T was from the lowest measured point up to 2.5 GeV/c (1.6 GeV/c) for Λ (K_S^0). The fitting functions were used to extrapolate the spectra to zero p_T to extract integrated particle yields dN/dy . The results are given in Table 1. The systematic uncertainties of the integrated yields were determined by shifting the data points of the spectra simultaneously within their individual systematic uncertainties and reapplying the fitting and integration procedure. In addition, an extrapolation uncertainty was estimated, by using alternative (polynomial, exponential and Lévy-Tsallis [28, 29]) functions fitted to the low-momentum part of the spectrum, and the corresponding difference in obtained values was added in quadrature.

The p_T dependence of the Λ/K_S^0 ratios, formed for each centrality interval by a division of the respective measured p_T spectra, is presented in Fig. 3 (left panel). For comparison, the same ratios measured in minimum bias pp collisions at $\sqrt{s} = 0.9$ [12] and 7 TeV [20] are plotted as well.

The Λ/K_S^0 ratios observed in pp events at $\sqrt{s} = 0.9$ and 7 TeV agree within uncertainties over the presented p_T range, and they bound in energy the Pb–Pb results reported here. The ratio measured in the most peripheral Pb–Pb collisions is compatible with the pp measurement, where there is a maximum of about 0.55 at $p_T \sim 2$ GeV/c. As the centrality of the Pb–Pb collisions increases, the maximum value

Table 1: Integrated yields, dN/dy , for Λ and K_S⁰ with uncertainties which are dominantly systematic. A blast-wave fit is used to extrapolate to zero p_T . Fractions of extrapolated yield are specified. Ratios of integrated yields, Λ/K_S^0 , for each centrality bin with the total uncertainty, mainly from systematic sources, are shown.

	0–5%	5–10%	10–20%	20–40%	40–60%	60–80%	80–90%
Λ $p_T < 0.6 \text{ GeV}/c$ frac.	26 ± 3	22 ± 2	17 ± 2	10 ± 1	3.8 ± 0.4	1.0 ± 0.1	0.21 ± 0.03
	10%	11%	12%	14%	18%	24%	32%
K _S ⁰ $p_T < 0.4 \text{ GeV}/c$ frac.	110 ± 10	90 ± 6	68 ± 5	39 ± 3	14 ± 1	3.9 ± 0.2	0.85 ± 0.09
	20%	21%	21%	23%	25%	31%	33%
Ratio $dN/dy \Lambda/K_S^0$	0.24 ± 0.02	0.24 ± 0.02	0.25 ± 0.02	0.25 ± 0.02	0.26 ± 0.03	0.25 ± 0.02	0.25 ± 0.02

of the ratio also increases and its position shifts towards higher momenta. The ratio peaks at a value of about 1.6 at $p_T \sim 3.2 \text{ GeV}/c$ for the most central Pb–Pb collisions. This observation may be contrasted to the ratio of the integrated Λ and K_S⁰ yields which does not change with centrality (Table 1). At momenta above $p_T \sim 7 \text{ GeV}/c$, the Λ/K_S^0 ratio is independent of collision centrality and p_T , within the uncertainties, and compatible with that measured in pp events.

A comparison with similar measurements performed by the STAR Collaboration in Au–Au collisions at $\sqrt{s_{\text{NN}}} = 200 \text{ GeV}$ is shown in Fig. 3 (right panel). Since the anti-baryon-to-baryon ratio at the LHC is consistent with unity for all transverse momenta [30, 31], the Λ/K_S^0 and $\bar{\Lambda}/K_S^0$ ratios are identical and we show only the former. The STAR Λ/K_S^0 and $\bar{\Lambda}/K_S^0$ ratios shown are constructed by dividing the corresponding p_T spectra taken from [21]. The quoted 15% p_T -independent feed-down contribution was subtracted from the Λ and $\bar{\Lambda}$ spectra. The shape of the distributions of Λ/K_S^0 and $\bar{\Lambda}/K_S^0$ are the same but they are offset by about 20% and have peak values around 10% higher, and respectively lower, than the ALICE data. This comparison between LHC and RHIC data shows that the position of the maximum shifts towards higher transverse momenta as the beam energy increases. It is also seen that the baryon enhancement in central nucleus–nucleus collisions at the LHC decreases less rapidly with p_T , and, at $p_T \sim 6 \text{ GeV}/c$, it is a factor of two higher compared with that at RHIC.

Also shown in the right panel of Fig. 3 is a hydrodynamical model calculation [22, 23, 24] for most central collisions, which describes the Λ/K_S^0 ratio up to p_T about 2 GeV/c rather well, but for higher p_T progressively deviates from the data. Such decoupling between the calculations and measurements is already seen in the comparison of p_T -spectra [27]. The agreement for other charged particles is improved when the hydrodynamical calculations are coupled to final-state re-scattering model [25]. Therefore it would be interesting to compare these data and their centrality evolution with such treatment. For higher p_T , a recombination model calculation [5] is presented (Fig. 3, right panel). It approximately reproduces the shape, but overestimates the baryon enhancement by about 15%. In the right panel of Fig. 3, we also show a comparison of the EPOS model calculations [26] with the current data. This model takes into account the interaction between jets and the hydrodynamically expanding medium and arrives at a good description of the data.

In conclusion, we note that the excess of baryons at intermediate p_T , exhibiting such a strong centrality dependence in Pb–Pb collisions at $\sqrt{s_{\text{NN}}} = 2.76 \text{ TeV}$, does not reveal itself in pp collisions at the center-of-mass energy up to $\sqrt{s} = 7 \text{ TeV}$. At $p_T > 7 \text{ GeV}/c$, the Λ/K_S^0 ratios measured in Pb–Pb events for different centralities all merge together and with the dependence observed in pp collisions. This agreement between collision systems suggests that the relative fragmentation into Λ and K_S⁰ hadrons at high p_T , even in central collisions, is vacuum-like and not modified by the medium. In future, it would be interesting to extend the measurements to higher transverse momenta to see whether the nuclear modification factor behaves in the same way as the one for charged particles [32].

As the collision energy and centrality increase, the maximum of the $\Lambda(\bar{\Lambda})/K_S^0$ ratio shifts towards higher p_T , which is in qualitative agreement with the effect of increased radial flow, as predicted in [4]. The ratio of integrated Λ and K_S⁰ yields does not, within uncertainties, change with centrality and is equal to that measured in pp collisions at 0.9 and 7 TeV. This suggests that the baryon enhancement at intermediate

p_T is predominantly due to a re-distribution of baryons and mesons over the momentum range rather than due to an additional baryon production channel progressively opening up in more central heavy-ion collisions. This centrality dependence may be challenging for theoretical models which try to disentangle the quark-recombination contributions from the radial-flow effect and which, in addition, will need to describe other particle spectra and their p_T -dependent ratios.

The width of the baryon enhancement peak increases with the beam energy. However, contrary to expectations [7], the effect at the LHC is still restricted to an intermediate-momentum range and is not observed at high p_T . This puts constraints on parameters of particle production models involving coalescence of quarks generated in hard parton interactions [33].

Qualitatively, the baryon enhancement presented here as p_T dependence of Λ/K_S^0 ratios, is described in the low- p_T region (below 2 GeV/c) by collective hydrodynamical radial flow. In the high- p_T region (above 7–8 GeV/c), it is very similar to pp results, indicating that there it is dominated by hard processes and fragmentation. Our data provide evidence for the need to include the effect of the hydrodynamical expansion of the medium formed in Pb–Pb collisions on the mechanisms of fragmentation and hadronization.

Acknowledgements

The ALICE collaboration would like to thank all its engineers and technicians for their invaluable contributions to the construction of the experiment and the CERN accelerator teams for the outstanding performance of the LHC complex.

The ALICE collaboration acknowledges the following funding agencies for their support in building and running the ALICE detector:

State Committee of Science, World Federation of Scientists (WFS) and Swiss Fonds Kidagan, Armenia; Conselho Nacional de Desenvolvimento Científico e Tecnológico (CNPq), Financiadora de Estudos e Projetos (FINEP), Fundação de Amparo à Pesquisa do Estado de São Paulo (FAPESP);

National Natural Science Foundation of China (NSFC), the Chinese Ministry of Education (CMOE) and the Ministry of Science and Technology of China (MSTC);

Ministry of Education and Youth of the Czech Republic;

Danish Natural Science Research Council, the Carlsberg Foundation and the Danish National Research Foundation;

The European Research Council under the European Community's Seventh Framework Programme; Helsinki Institute of Physics and the Academy of Finland;

French CNRS-IN2P3, the ‘Region Pays de Loire’, ‘Region Alsace’, ‘Region Auvergne’ and CEA, France;

German BMBF and the Helmholtz Association;

General Secretariat for Research and Technology, Ministry of Development, Greece;

Hungarian OTKA and National Office for Research and Technology (NKTH);

Department of Atomic Energy and Department of Science and Technology of the Government of India; Istituto Nazionale di Fisica Nucleare (INFN) and Centro Fermi - Museo Storico della Fisica e Centro Studi e Ricerche “Enrico Fermi”, Italy;

MEXT Grant-in-Aid for Specially Promoted Research, Japan;

Joint Institute for Nuclear Research, Dubna;

National Research Foundation of Korea (NRF);

CONACYT, DGAPA, México, ALFA-EC and the EPLANET Program (European Particle Physics Latin American Network)

Stichting voor Fundamenteel Onderzoek der Materie (FOM) and the Nederlandse Organisatie voor Wetenschappelijk Onderzoek (NWO), Netherlands;

Research Council of Norway (NFR);

Polish Ministry of Science and Higher Education;
 National Authority for Scientific Research - NASR (Autoritatea Națională pentru Cercetare Științifică - ANCS);
 Ministry of Education and Science of Russian Federation, Russian Academy of Sciences, Russian Federal Agency of Atomic Energy, Russian Federal Agency for Science and Innovations and The Russian Foundation for Basic Research;
 Ministry of Education of Slovakia;
 Department of Science and Technology, South Africa;
 CIEMAT, EELA, Ministerio de Economía y Competitividad (MINECO) of Spain, Xunta de Galicia (Consellería de Educación), CEADEN, Cubaenergía, Cuba, and IAEA (International Atomic Energy Agency);
 Swedish Research Council (VR) and Knut & Alice Wallenberg Foundation (KAW);
 Ukraine Ministry of Education and Science;
 United Kingdom Science and Technology Facilities Council (STFC);
 The United States Department of Energy, the United States National Science Foundation, the State of Texas, and the State of Ohio.

References

- [1] S. S. Adler *et al.* (PHENIX Collaboration), Phys. Rev. Lett. **91**, 172301 (2003).
- [2] J. Adams *et al.* (STAR Collaboration), (2006), arXiv:nucl-ex/0601042 .
- [3] T. Schuster *et al.* (NA49 Collaboration), J.Phys. **G32**, S479 (2006), arXiv:nucl-ex/0606005 .
- [4] R. Fries and B. Müller, Eur. Phys. J. C **34**, S279 (2004).
- [5] R. J. Fries, V. Greco, and P. Sorensen, Ann. Rev. Nucl. Part. Sci. **58**, 177 (2008), arXiv:nucl-th/0807.4939 .
- [6] R. C. Hwa and C. Yang, Phys. Rev. C **70**, 024905 (2004), arXiv:nucl-th/0401001 .
- [7] R. C. Hwa, J. Phys. G. **35**, 104017 (2008), arXiv:nucl-th/0804.3763 .
- [8] M. Lamont (STAR Collaboration), Eur. Phys. J. C **49**, 35 (2007).
- [9] K. Aamodt *et al.* (ALICE Collaboration), JINST **3**, S08002 (2008).
- [10] B. Abelev *et al.* (ALICE Collaboration), (2013), arXiv:nucl-ex/1301.4361 .
- [11] J. Beringer *et al.* (Particle Data Group), Phys. Rev. D **86**, 010001 (2012).
- [12] K. Aamodt *et al.* (ALICE Collaboration), Eur. Phys. J. C **71**, 1594 (2011).
- [13] J. Podolanski and R. Armenteros, Phil. Mag. **45**, 13 (1954).
- [14] M. Gyulassy and X.-N. Wang, Comp. Phys. Comm. **83**, 307 (1994), arXiv:nucl-th/9502021 .
- [15] R. Brun, F. Carminati, and S. Giani, (1994), CERN Program Library Long Writeup.
- [16] ALICE, *Technical Design Report for the ALICE Computing, CERN/LHCC 2005-18; AliRoot, ALICE Offline simulation, reconstruction and analysis framework*, Tech. Rep. (2005).
- [17] B. Abelev *et al.* (ALICE Collaboration), (2013), to be published .
- [18] M. Nicassio (for the ALICE Collaboration), Acta Phys. Polon. B Proc. Supp. **5**, 237 (2012).

- [19] E. Schnedermann, J. Sollfrank, and U. W. Heinz, Phys. Rev. C **48**, 2462 (1993), arXiv:nucl-th/9307020 .
- [20] B. Abelev *et al.* (ALICE Collaboration), (2013), to be published .
- [21] G. Agakishiev *et al.* (STAR Collaboration), Phys. Rev. Lett. **108**, 072301 (2012), arXiv:nucl-ex/1107.2955 .
- [22] H. Song and U. W. Heinz, Phys. Lett. **B658**, 279 (2008), arXiv:nucl-th/0709.0742 .
- [23] H. Song and U. W. Heinz, Phys. Rev. **C77**, 064901 (2008), arXiv:nucl-th/0712.3715 .
- [24] H. Song and U. W. Heinz, Phys. Rev. **C78**, 024902 (2008), arXiv:nucl-th/0805.1756 .
- [25] H. Song, S. A. Bass, and U. Heinz, Phys. Rev. **C83**, 054912 (2011), arXiv:nucl-th/1103.2380 .
- [26] K. Werner, Phys. Rev. Lett. **109**, 102301 (2012).
- [27] B. Abelev *et al.* (ALICE Collaboration), arXiv:hep-ex/1303.0737 .
- [28] C. Tsallis, J. Stat. Phys. **52**, 479 (1988).
- [29] B. Abelev *et al.* (STAR Collaboration), Phys. Rev. **C75**, 064901 (2007), arXiv:nucl-ex/0607033 .
- [30] K. Aamodt *et al.* (ALICE Collaboration), Phys. Rev. Lett. **105**, 072002 (2010), arXiv:nucl-ex/1006.5432 .
- [31] B. Abelev *et al.* (ALICE Collaboration), Phys. Rev. Lett. **109**, 252301 (2012).
- [32] K. Aamodt *et al.* (ALICE Collaboration), Physics Letters B **696**, 30 (2011).
- [33] R. C. Hwa and L. Zhu, arXiv:nucl-th/1202.2091 .

A The ALICE Collaboration

- B. Abelev⁶⁹, J. Adam³⁶, D. Adamová⁷⁷, A.M. Adare¹²⁵, M.M. Aggarwal⁸¹, G. Aglieri Rinella³³, M. Agnello^{87,104}, A.G. Agocs¹²⁴, A. Agostinelli²⁵, Z. Ahammed¹²⁰, N. Ahmad¹⁶, A. Ahmad Masoodi¹⁶, I. Ahmed¹⁴, S.U. Ahn⁶², S.A. Ahn⁶², I. Aimo^{104,87}, S. Aiola¹²⁵, M. Ajaz¹⁴, A. Akindinov⁵³, D. Aleksandrov⁹³, B. Alessandro¹⁰⁴, D. Alexandre⁹⁵, A. Alici^{11,98}, A. Alkin³, J. Alme³⁴, T. Alt³⁸, V. Altini³⁰, S. Altinpinar¹⁷, I. Altsybeev¹¹⁹, C. Alves Garcia Prado¹¹¹, C. Andrei⁷², A. Andronic⁹⁰, V. Anguelov⁸⁶, J. Anielski⁴⁸, T. Antičić⁹¹, F. Antinori¹⁰¹, P. Antonioli⁹⁸, L. Aphectche¹⁰⁵, H. Appelshäuser⁴⁶, N. Arbor⁶⁵, S. Arcelli²⁵, N. Armesto¹⁵, R. Arnaldi¹⁰⁴, T. Aronsson¹²⁵, I.C. Arsene⁹⁰, M. Arslanbek⁴⁶, A. Augustinus³³, R. Averbeck⁹⁰, T.C. Awes⁷⁸, M.D. Azmi⁸³, M. Bach³⁸, A. Badalà¹⁰⁰, Y.W. Baek^{64,39}, R. Bailhache⁴⁶, V. Bairathi⁸⁵, R. Bala^{104,84}, A. Baldissari¹³, F. Baltasar Dos Santos Pedrosa³³, J. Bán⁵⁴, R.C. Baral⁵⁶, R. Barbera²⁶, F. Barile³⁰, G.G. Barnaföldi¹²⁴, L.S. Barnby⁹⁵, V. Barret⁶⁴, J. Bartke¹⁰⁸, M. Basile²⁵, N. Bastid⁶⁴, S. Basu¹²⁰, B. Bathen⁴⁸, G. Batigne¹⁰⁵, B. Batyunya⁶¹, P.C. Batzinger²⁰, C. Baumann⁴⁶, I.G. Bearden⁷⁴, H. Beck⁴⁶, N.K. Behera⁴², I. Belikov⁴⁹, F. Bellini²⁵, R. Bellwied¹¹³, E. Belmont-Moreno⁵⁹, G. Bencedi¹²⁴, S. Beole²³, I. Berceanu⁷², A. Bercuci⁷², Y. Berdnikov⁷⁹, D. Berenyi¹²⁴, A.A.E. Bergognon¹⁰⁵, R.A. Bertens⁵², D. Berzana²³, L. Betev³³, A. Bhasin⁸⁴, A.K. Bhati⁸¹, J. Bhom¹¹⁷, L. Bianchi²³, N. Bianchi⁶⁶, J. Bielčík³⁶, J. Bielčíková⁷⁷, A. Bilandžić⁷⁴, S. Bjelogrlic⁵², F. Blanco⁹, F. Blanco¹¹³, D. Blau⁹³, C. Blume⁴⁶, F. Bock^{68,86}, A. Bogdanov⁷⁰, H. Bøggild⁷⁴, M. Bogolyubsky⁵⁰, L. Boldizsár¹²⁴, M. Bombara³⁷, J. Book⁴⁶, H. Borel¹³, A. Borissov¹²³, J. Bornschein³⁸, M. Botje⁷⁵, E. Botta²³, S. Böttger⁴⁵, P. Braun-Munzinger⁹⁰, M. Bregant¹⁰⁵, T. Breitner⁴⁵, T.A. Broker⁴⁶, T.A. Browning⁸⁸, M. Broz³⁵, R. Brun³³, E. Bruna¹⁰⁴, G.E. Bruno³⁰, D. Budnikov⁹², H. Buesching⁴⁶, S. Bufalino¹⁰⁴, P. Buncic³³, O. Busch⁸⁶, Z. Buthelezi⁶⁰, D. Caffarrì²⁷, X. Cai⁶, H. Caines¹²⁵, A. Caliva⁵², E. Calvo Villar⁹⁶, P. Camerini²², V. Canoa Roman^{10,33}, G. Cara Romeo⁹⁸, F. Carena³³, W. Carena³³, F. Carminati³³, A. Casanova Díaz⁶⁶, J. Castillo Castellanos¹³, E.A.R. Casula²¹, V. Catanescu⁷², C. Cavicchioli³³, C. Ceballos Sanchez⁸, J. Cepila³⁶, P. Cerello¹⁰⁴, B. Chang¹¹⁴, S. Chapelard³³, J.L. Charvet¹³, S. Chattopadhyay¹²⁰, S. Chattopadhyay⁹⁴, M. Cherney⁸⁰, C. Cheshkov¹¹⁸, B. Cheynis¹¹⁸, V. Chibante Barroso³³, D.D. Chinellato¹¹³, P. Chochula³³, M. Chojnacki⁷⁴, S. Choudhury¹²⁰, P. Christakoglou⁷⁵, C.H. Christensen⁷⁴, P. Christiansen³¹, T. Chujo¹¹⁷, S.U. Chung⁸⁹, C. Cicalo⁹⁹, L. Cifarelli^{11,25}, F. Cindolo⁹⁸, J. Cleymans⁸³, F. Colamaria³⁰, D. Colella³⁰, A. Collu²¹, M. Colocci²⁵, G. Conesa Balbastre⁶⁵, Z. Conesa del Valle^{44,33}, M.E. Connors¹²⁵, G. Contin²², J.G. Contreras¹⁰, T.M. Cormier¹²³, Y. Corrales Morales²³, P. Cortese²⁹, I. Cortés Maldonado², M.R. Cosentino⁶⁸, F. Costa³³, P. Crochet⁶⁴, R. Cruz Albino¹⁰, E. Cuautle⁵⁸, L. Cunqueiro⁶⁶, A. Dainese¹⁰¹, R. Dang⁶, A. Danu⁵⁷, K. Das⁹⁴, D. Das⁹⁴, I. Das⁴⁴, A. Dash¹¹², S. Dash⁴², S. De¹²⁰, H. Delagrange¹⁰⁵, A. Deloff⁷¹, E. Dénes¹²⁴, A. Deppman¹¹¹, G.O.V. de Barros¹¹¹, A. De Caro^{11,28}, G. de Cataldo⁹⁷, J. de Cuveland³⁸, A. De Falco²¹, D. De Gruttola^{28,11}, N. De Marco¹⁰⁴, S. De Pasquale²⁸, R. de Rooij⁵², M.A. Diaz Corchero⁹, T. Dietel⁴⁸, R. Divià³³, D. Di Bari³⁰, C. Di Giglio³⁰, S. Di Liberto¹⁰², A. Di Mauro³³, P. Di Nezza⁶⁶, Ø. Djupsland¹⁷, A. Dobrin^{52,123}, T. Dobrowolski⁷¹, B. Döningus^{90,46}, O. Dordic²⁰, A.K. Dubey¹²⁰, A. Dubla⁵², L. Ducroux¹¹⁸, P. Dupieux⁶⁴, A.K. Dutta Majumdar⁹⁴, G. D Erasmo³⁰, D. Elia⁹⁷, D. Emschermann⁴⁸, H. Engel⁴⁵, B. Erazmus^{33,105}, H.A. Erdal³⁴, D. Eschweiler³⁸, B. Espagnon⁴⁴, M. Estienne¹⁰⁵, S. Esumi¹¹⁷, D. Evans⁹⁵, S. Evdokimov⁵⁰, G. Eyyubova²⁰, D. Fabris¹⁰¹, J. Faivre⁶⁵, D. Falchieri²⁵, A. Fantoni⁶⁶, M. Fasel⁸⁶, D. Fehlker¹⁷, L. Feldkamp⁴⁸, D. Felea⁵⁷, A. Feliciello¹⁰⁴, G. Feofilov¹¹⁹, J. Ferencei⁷⁷, A. Fernández Téllez², E.G. Ferreiro¹⁵, A. Ferretti²³, A. Festanti²⁷, J. Figiel¹⁰⁸, M.A.S. Figueiredo¹¹¹, S. Filchagin⁹², D. Finogeev⁵¹, F.M. Fionda³⁰, E.M. Fiore³⁰, E. Floratos⁸², M. Floris³³, S. Foertsch⁶⁰, P. Foka⁹⁰, S. Fokin⁹³, E. Fragiocomo¹⁰³, A. Francescon^{27,33}, U. Frankenfeld⁹⁰, U. Fuchs³³, C. Furget⁶⁵, M. Fusco Girard²⁸, J.J. Gaardhøje⁷⁴, M. Gagliardi²³, A. Gago⁹⁶, M. Gallio²³, D.R. Gangadharan¹⁸, P. Ganoti⁷⁸, C. Garabatos⁹⁰, E. Garcia-Solis¹², C. Gargiulo³³, I. Garishvili⁶⁹, J. Gerhard³⁸, M. Germain¹⁰⁵, A. Gheata³³, M. Gheata^{33,57}, B. Ghidini³⁰, P. Ghosh¹²⁰, P. Gianotti⁶⁶, P. Giubellino³³, E. Gladysz-Dziadus¹⁰⁸, P. Glässel⁸⁶, L. Goerlich¹⁰⁸, R. Gomez^{10,110}, P. González-Zamora⁹, S. Gorbunov³⁸, S. Gotovac¹⁰⁷, L.K. Graczykowski¹²², R. Grajcarek⁸⁶, A. Grelli⁵², C. Grigoras³³, A. Grigoras³³, V. Grigoriev⁷⁰, A. Grigoryan¹, S. Grigoryan⁶¹, B. Grinyov³, N. Grion¹⁰³, J.F. Grosse-Oetringhaus³³, J.-Y. Grossiord¹¹⁸, R. Grossiord³³, F. Guber⁵¹, R. Guernane⁶⁵, B. Guerzoni²⁵, M. Guilbaud¹¹⁸, K. Gulbrandsen⁷⁴, H. Gulkanyan¹, T. Gunji¹¹⁶, A. Gupta⁸⁴, R. Gupta⁸⁴, K. H. Khan¹⁴, R. Haake⁴⁸, Ø. Haaland¹⁷, C. Hadjidakis⁴⁴, M. Haiduc⁵⁷, H. Hamagaki¹¹⁶, G. Hamar¹²⁴, L.D. Hanratty⁹⁵, A. Hansen⁷⁴, J.W. Harris¹²⁵, H. Hartmann³⁸, A. Harton¹², D. Hatzifotiadou⁹⁸, S. Hayashi¹¹⁶, A. Hayrapetyan^{33,1}, S.T. Heckel⁴⁶, M. Heide⁴⁸, H. Helstrup³⁴, A. Hergelegiu⁷², G. Herrera Corral¹⁰, N. Herrmann⁸⁶, B.A. Hess³², K.F. Hetland³⁴, B. Hicks¹²⁵, B. Hippolyte⁴⁹, Y. Hori¹¹⁶, P. Hristov³³, I. Hřivnáčová⁴⁴, M. Huang¹⁷, T.J. Humanic¹⁸, D. Hutter³⁸, D.S. Hwang¹⁹, R. Ilkaev⁹², I. Ilkiv⁷¹, M. Inaba¹¹⁷, E. Incani²¹, G.M. Innocenti²³, C. Ionita³³, M. Ippolitov⁹³, M. Irfan¹⁶, M. Ivanov⁹⁰, V. Ivanov⁷⁹,

O. Ivanytskyi³, A. Jachołkowski²⁶, C. Jahnke¹¹¹, H.J. Jang⁶², M.A. Janik¹²², P.H.S.Y. Jayarathna¹¹³, S. Jena^{42,113}, R.T. Jimenez Bustamante⁵⁸, P.G. Jones⁹⁵, H. Jung³⁹, A. Jusko⁹⁵, S. Kalcher³⁸, P. Kaliňák⁵⁴, A. Kalweit³³, J.H. Kang¹²⁶, V. Kaplin⁷⁰, S. Kar¹²⁰, A. Karasu Uysal⁶³, O. Karavichev⁵¹, T. Karavicheva⁵¹, E. Karpechev⁵¹, A. Kazantsev⁹³, U. Kebschull⁴⁵, R. Keidel¹²⁷, B. Ketzer⁴⁶, M.M. Khan¹⁶, P. Khan⁹⁴, S.A. Khan¹²⁰, A. Khanzadeev⁷⁹, Y. Kharlov⁵⁰, B. Kileng³⁴, T. Kim¹²⁶, B. Kim¹²⁶, D.J. Kim¹¹⁴, D.W. Kim^{39,62}, J.S. Kim³⁹, M. Kim³⁹, M. Kim¹²⁶, S. Kim¹⁹, S. Kirsch³⁸, I. Kisel³⁸, S. Kiselev⁵³, A. Kisiel¹²², G. Kiss¹²⁴, J.L. Klay⁵, J. Klein⁸⁶, C. Klein-Bösing⁴⁸, A. Kluge³³, M.L. Knichel⁹⁰, A.G. Knospe¹⁰⁹, C. Kobdaj^{33,106}, M.K. Köhler⁹⁰, T. Kollegger³⁸, A. Kolojvari¹¹⁹, V. Kondratiev¹¹⁹, N. Kondratyeva⁷⁰, A. Konevskikh⁵¹, V. Kovalenko¹¹⁹, M. Kowalski¹⁰⁸, S. Kox⁶⁵, G. Koyithatta Meethaleveedu⁴², J. Kral¹¹⁴, I. Králik⁵⁴, F. Kramer⁴⁶, A. Kravčáková³⁷, M. Krelina³⁶, M. Kretz³⁸, M. Krivda^{54,95}, F. Krizek^{36,77,40}, M. Krus³⁶, E. Kryshen⁷⁹, M. Krzewicki⁹⁰, V. Kucera⁷⁷, Y. Kucheriaev⁹³, T. Kugathasan³³, C. Kuhn⁴⁹, P.G. Kuijer⁷⁵, I. Kulakov⁴⁶, J. Kumar⁴², P. Kurashvili⁷¹, A.B. Kurepin⁵¹, A. Kurepin⁵¹, A. Kuryakin⁹², V. Kushpil⁷⁷, S. Kushpil⁷⁷, M.J. Kweon⁸⁶, Y. Kwon¹²⁶, P. Ladrón de Guevara⁵⁸, C. Lagana Fernandes¹¹¹, I. Lakomov⁴⁴, R. Langoy¹²¹, C. Lara⁴⁵, A. Lardeux¹⁰⁵, A. Lattuca²³, S.L. La Pointe⁵², P. La Rocca²⁶, R. Lea²², M. Lechman³³, S.C. Lee³⁹, G.R. Lee⁹⁵, I. Legrand³³, J. Lehnert⁴⁶, R.C. Lemmon⁷⁶, M. Lenhardt⁹⁰, V. Lenti⁹⁷, M. Leoncino²³, I. León Monzón¹¹⁰, P. Lévai¹²⁴, S. Li^{64,6}, J. Lien^{121,17}, R. Lietava⁹⁵, S. Lindal²⁰, V. Lindenstruth³⁸, C. Lippmann⁹⁰, M.A. Lisa¹⁸, H.M. Ljunggren³¹, D.F. Lodato⁵², P.I. Loenne¹⁷, V.R. Loggins¹²³, V. Loginov⁷⁰, D. Lohner⁸⁶, C. Loizides⁶⁸, X. Lopez⁶⁴, E. López Torres⁸, G. Løvhøiden²⁰, X.-G. Lu⁸⁶, P. Luettig⁴⁶, M. Lunardon²⁷, J. Luo⁶, G. Luparello⁵², C. Luzzi³³, P. M. Jacobs⁶⁸, R. Ma¹²⁵, A. Maevskaya⁵¹, M. Mager³³, D.P. Mahapatra⁵⁶, A. Maire⁸⁶, M. Malaev⁷⁹, I. Maldonado Cervantes⁵⁸, L. Malinina^{61,ii}, D. Mal'Kevich⁵³, P. Malzacher⁹⁰, A. Mamonov⁹², L. Manceau¹⁰⁴, V. Manko⁹³, F. Manso⁶⁴, V. Manzari^{97,33}, M. Marchisone^{64,23}, J. Mareš⁵⁵, G.V. Margagliotti²², A. Margotti⁹⁸, A. Marín⁹⁰, C. Markert^{33,109}, M. Marquard⁴⁶, I. Martashvili¹¹⁵, N.A. Martin⁹⁰, P. Martinengo³³, M.I. Martínez², G. Martínez García¹⁰⁵, J. Martin Blanco¹⁰⁵, Y. Martynov³, A. Mas¹⁰⁵, S. Masciocchi⁹⁰, M. Masera²³, A. Masoni⁹⁹, L. Massacrier¹⁰⁵, A. Mastroserio³⁰, A. Matyja¹⁰⁸, J. Mazer¹¹⁵, R. Mazumder⁴³, M.A. Mazzoni¹⁰², F. Meddi²⁴, A. Menchaca-Rocha⁵⁹, J. Mercado Pérez⁸⁶, M. Meres³⁵, Y. Miake¹¹⁷, K. Mikhaylov^{53,61}, L. Milano^{23,33}, J. Milosevic^{20,iii}, A. Mischke⁵², A.N. Mishra⁴³, D. Miśkowiec⁹⁰, C. Mitu⁵⁷, J. Mlynarz¹²³, B. Mohanty^{73,120}, L. Molnar^{49,124}, L. Montaño Zetina¹⁰, M. Monteno¹⁰⁴, E. Montes⁹, M. Morando²⁷, D.A. Moreira De Godoy¹¹¹, S. Moretto²⁷, A. Morreale¹¹⁴, A. Morsch³³, V. Muccifora⁶⁶, E. Mudnic¹⁰⁷, S. Muhuri¹²⁰, M. Mukherjee¹²⁰, H. Müller³³, M.G. Munhoz¹¹¹, S. Murray⁶⁰, L. Musa³³, B.K. Nandi⁴², R. Nania⁹⁸, E. Nappi⁹⁷, C. Nattrass¹¹⁵, T.K. Nayak¹²⁰, S. Nazarenko⁹², A. Nedosekin⁵³, M. Nicassio^{90,30}, M. Niculescu^{33,57}, B.S. Nielsen⁷⁴, S. Nikolaev⁹³, S. Nikulin⁹³, V. Nikulin⁷⁹, B.S. Nilsen⁸⁰, M.S. Nilsson²⁰, F. Noferini^{11,98}, P. Nomokonov⁶¹, G. Nooren⁵², A. Nyanin⁹³, A. Nyatha⁴², J. Nystrand¹⁷, H. Oeschler^{86,47}, S.K. Oh^{39,iv}, S. Oh¹²⁵, L. Olah¹²⁴, J. Oleniacz¹²², A.C. Oliveira Da Silva¹¹¹, J. Onderwaater⁹⁰, C. Oppedisano¹⁰⁴, A. Ortiz Velasquez³¹, A. Oskarsson³¹, J. Otwinowski⁹⁰, K. Oyama⁸⁶, Y. Pachmayer⁸⁶, M. Pachr³⁶, P. Pagano²⁸, G. Paić⁵⁸, F. Painke³⁸, C. Pajares¹⁵, S.K. Pal¹²⁰, A. Palaha⁹⁵, A. Palmeri¹⁰⁰, V. Papikyan¹, G.S. Pappalardo¹⁰⁰, W.J. Park⁹⁰, A. Passfeld⁴⁸, D.I. Patalakha⁵⁰, V. Paticchio⁹⁷, B. Paul⁹⁴, T. Pawlak¹²², T. Peitzmann⁵², H. Pereira Da Costa¹³, E. Pereira De Oliveira Filho¹¹¹, D. Peresunko⁹³, C.E. Pérez Lara⁷⁵, D. Perrino³⁰, W. Peryt^{122,i}, A. Pesci⁹⁸, Y. Pestov⁴, V. Petráček³⁶, M. Petran³⁶, M. Petris⁷², P. Petrov⁹⁵, M. Petrovici⁷², C. Petta²⁶, S. Piano¹⁰³, M. Pikna³⁵, P. Pillot¹⁰⁵, O. Pinazza^{33,98}, L. Pinsky¹¹³, N. Pitz⁴⁶, D.B. Piyarathna¹¹³, M. Planinic⁹¹, M. Płoskon⁶⁸, J. Pluta¹²², S. Pochybova¹²⁴, P.L.M. Podesta-Lerma¹¹⁰, M.G. Poghosyan³³, B. Polichtchouk⁵⁰, A. Pop⁷², S. Porteboeuf-Houssais⁶⁴, V. Pospíšil³⁶, B. Potukuchi⁸⁴, S.K. Prasad¹²³, R. Preghenella^{11,98}, F. Prino¹⁰⁴, C.A. Pruneau¹²³, I. Pshenichnov⁵¹, G. Puddu²¹, V. Punin⁹², J. Putschke¹²³, H. Qvigstad²⁰, A. Rachevski¹⁰³, A. Rademakers³³, J. Rak¹¹⁴, A. Rakotozafindrabe¹³, L. Ramello²⁹, S. Raniwala⁸⁵, R. Raniwala⁸⁵, S.S. Räsänen⁴⁰, B.T. Rascanu⁴⁶, D. Rathee⁸¹, W. Rauch³³, A.W. Rauf¹⁴, V. Razazi²¹, K.F. Read¹¹⁵, J.S. Real⁶⁵, K. Redlich^{71,v}, R.J. Reed¹²⁵, A. Rehman¹⁷, P. Reichelt⁴⁶, M. Reicher⁵², F. Reidt^{33,86}, R. Renfordt⁴⁶, A.R. Reolon⁶⁶, A. Reshetin⁵¹, F. Rettig³⁸, J.-P. Revol³³, K. Reygers⁸⁶, L. Riccati¹⁰⁴, R.A. Ricci⁶⁷, T. Richert³¹, M. Richter²⁰, P. Riedler³³, W. Riegler³³, F. Riggi²⁶, A. Rivetti¹⁰⁴, M. Rodríguez Cahuantzi², A. Rodriguez Manso⁷⁵, K. Røed^{17,20}, E. Rogochaya⁶¹, S. Rohni⁸⁴, D. Rohr³⁸, D. Röhrich¹⁷, R. Romita^{76,90}, F. Ronchetti⁶⁶, P. Rosnet⁶⁴, S. Rossegger³³, A. Rossi³³, P. Roy⁹⁴, C. Roy⁴⁹, A.J. Rubio Montero⁹, R. Rui²², R. Russo²³, E. Ryabinkin⁹³, A. Rybicki¹⁰⁸, S. Sadovsky⁵⁰, K. Šafářk³³, R. Sahoo⁴³, P.K. Sahu⁵⁶, J. Saini¹²⁰, H. Sakaguchi⁴¹, S. Sakai^{68,66}, D. Sakata¹¹⁷, C.A. Salgado¹⁵, J. Salzwedel¹⁸, S. Sambyal⁸⁴, V. Samsonov⁷⁹, X. Sanchez Castro^{58,49}, L. Šádor⁵⁴, A. Sandoval⁵⁹, M. Sano¹¹⁷, G. Santagati²⁶, R. Santoro^{11,33}, D. Sarkar¹²⁰, E. Scapparone⁹⁸, F. Scarlassara²⁷, R.P. Scharenberg⁸⁸, C. Schiaua⁷², R. Schicker⁸⁶, C. Schmidt⁹⁰, H.R. Schmidt³², S. Schuchmann⁴⁶,

J. Schukraft³³, M. Schulc³⁶, T. Schuster¹²⁵, Y. Schutz^{33,105}, K. Schwarz⁹⁰, K. Schweda⁹⁰, G. Scioli²⁵, E. Scomparin¹⁰⁴, R. Scott¹¹⁵, P.A. Scott⁹⁵, G. Segato²⁷, I. Selyuzhenkov⁹⁰, J. Seo⁸⁹, S. Serici²¹, E. Serradilla^{9,59}, A. Sevcenco⁵⁷, A. Shabetai¹⁰⁵, G. Shabratova⁶¹, R. Shahoyan³³, S. Sharma⁸⁴, N. Sharma¹¹⁵, K. Shigaki⁴¹, K. Shtejer⁸, Y. Sibiriak⁹³, S. Siddhanta⁹⁹, T. Siemiaczuk⁷¹, D. Silvermyr⁷⁸, C. Silvestre⁶⁵, G. Simatovic⁹¹, R. Singaraju¹²⁰, R. Singh⁸⁴, S. Singha¹²⁰, V. Singhal¹²⁰, B.C. Sinha¹²⁰, T. Sinha⁹⁴, B. Sitar³⁵, M. Sitta²⁹, T.B. Skaali²⁰, K. Skjerdal¹⁷, R. Smakal³⁶, N. Smirnov¹²⁵, R.J.M. Snellings⁵², R. Soltz⁶⁹, M. Song¹²⁶, J. Song⁸⁹, C. Soos³³, F. Soramel²⁷, M. Spacek³⁶, I. Sputowska¹⁰⁸, M. Spyropoulou-Stassinaki⁸², B.K. Srivastava⁸⁸, J. Stachel⁸⁶, I. Stan⁵⁷, G. Stefanek⁷¹, M. Steinpreis¹⁸, E. Stenlund³¹, G. Steyn⁶⁰, J.H. Stiller⁸⁶, D. Stocco¹⁰⁵, M. Stolpovskiy⁵⁰, P. Strmen³⁵, A.A.P. Suade¹¹¹, M.A. Subieta Vásquez²³, T. Sugitate⁴¹, C. Suire⁴⁴, M. Suleymanov¹⁴, R. Sultanov⁵³, M. Šumbera⁷⁷, T. Susa⁹¹, T.J.M. Symons⁶⁸, A. Szanto de Toledo¹¹¹, I. Szarka³⁵, A. Szczepankiewicz³³, M. Szymański¹²², J. Takahashi¹¹², M.A. Tangaro³⁰, J.D. Tapia Takaki⁴⁴, A. Tarantola Peloni⁴⁶, A. Tarazona Martinez³³, A. Tauro³³, G. Tejeda Muñoz², A. Telesca³³, C. Terrevoli³⁰, A. Ter Minasyan^{93,70}, J. Thäder⁹⁰, D. Thomas⁵², R. Tieulent¹¹⁸, A.R. Timmins¹¹³, A. Toia¹⁰¹, H. Torii¹¹⁶, V. Trubnikov³, W.H. Trzaska¹¹⁴, T. Tsuji¹¹⁶, A. Tumkin⁹², R. Turrisi¹⁰¹, T.S. Tveter²⁰, J. Ulery⁴⁶, K. Ullaland¹⁷, J. Ulrich⁴⁵, A. Uras¹¹⁸, G.M. Urciuoli¹⁰², G.L. Usai²¹, M. Vajzer⁷⁷, M. Vala^{54,61}, L. Valencia Palomo⁴⁴, P. Vande Vyvre³³, L. Vannucci⁶⁷, J.W. Van Hoorne³³, M. van Leeuwen⁵², A. Vargas², R. Varma⁴², M. Vasileiou⁸², A. Vasiliev⁹³, V. Vechernin¹¹⁹, M. Veldhoen⁵², M. Venaruzzo²², E. Vercellin²³, S. Vergara², R. Vernet⁷, M. Verweij^{123,52}, L. Vickovic¹⁰⁷, G. Viesti²⁷, J. Viinikainen¹¹⁴, Z. Vilakazi⁶⁰, O. Villalobos Baillie⁹⁵, A. Vinogradov⁹³, L. Vinogradov¹¹⁹, Y. Vinogradov⁹², T. Virgili²⁸, Y.P. Viyogi¹²⁰, A. Vodopyanov⁶¹, M.A. Völk⁸⁶, S. Voloshin¹²³, K. Voloshin⁵³, G. Volpe³³, B. von Haller³³, I. Vorobyev¹¹⁹, D. Vranic^{33,90}, J. Vrláková³⁷, B. Vulpescu⁶⁴, A. Vyushin⁹², B. Wagner¹⁷, V. Wagner³⁶, J. Wagner⁹⁰, Y. Wang⁸⁶, Y. Wang⁶, M. Wang⁶, D. Watanabe¹¹⁷, K. Watanabe¹¹⁷, M. Weber¹¹³, J.P. Wessels⁴⁸, U. Westerhoff⁴⁸, J. Wiechula³², J. Wikne²⁰, M. Wilde⁴⁸, G. Wilk⁷¹, J. Wilkinson⁸⁶, M.C.S. Williams⁹⁸, B. Windelband⁸⁶, M. Winn⁸⁶, C. Xiang⁶, C.G. Yaldo¹²³, Y. Yamaguchi¹¹⁶, H. Yang^{13,52}, P. Yang⁶, S. Yang¹⁷, S. Yano⁴¹, S. Yasnopolskiy⁹³, J. Yi⁸⁹, Z. Yin⁶, I.-K. Yoo⁸⁹, I. Yushmanov⁹³, V. Zaccolo⁷⁴, C. Zach³⁶, C. Zampolli⁹⁸, S. Zaporozhets⁶¹, A. Zarochentsev¹¹⁹, P. Závada⁵⁵, N. Zaviyalov⁹², H. Zbroszczyk¹²², P. Zelnicek⁴⁵, I.S. Zgura⁵⁷, M. Zhalov⁷⁹, F. Zhang⁶, Y. Zhang⁶, H. Zhang⁶, X. Zhang^{68,64,6}, D. Zhou⁶, Y. Zhou⁵², F. Zhou⁶, X. Zhu⁶, J. Zhu⁶, J. Zhu⁶, H. Zhu⁶, A. Zichichi^{11,25}, M.B. Zimmermann^{48,33}, A. Zimmermann⁸⁶, G. Zinovjev³, Y. Zoccarato¹¹⁸, M. Zynovyev³, M. Zyzak⁴⁶

Affiliation notes

ⁱ Deceased

ⁱⁱ Also at: M.V.Lomonosov Moscow State University, D.V.Skobeltsyn Institute of Nuclear Physics, Moscow, Russia

ⁱⁱⁱ Also at: University of Belgrade, Faculty of Physics and "Vinča" Institute of Nuclear Sciences, Belgrade, Serbia

^{iv} Permanent address: Konkuk University, Seoul, Korea

^v Also at: Institute of Theoretical Physics, University of Wroclaw, Wroclaw, Poland

Collaboration Institutes

- ¹ A. I. Alikhanyan National Science Laboratory (Yerevan Physics Institute) Foundation, Yerevan, Armenia
- ² Benemérita Universidad Autónoma de Puebla, Puebla, Mexico
- ³ Bogolyubov Institute for Theoretical Physics, Kiev, Ukraine
- ⁴ Budker Institute for Nuclear Physics, Novosibirsk, Russia
- ⁵ California Polytechnic State University, San Luis Obispo, California, United States
- ⁶ Central China Normal University, Wuhan, China
- ⁷ Centre de Calcul de l'IN2P3, Villeurbanne, France
- ⁸ Centro de Aplicaciones Tecnológicas y Desarrollo Nuclear (CEADEN), Havana, Cuba
- ⁹ Centro de Investigaciones Energéticas Medioambientales y Tecnológicas (CIEMAT), Madrid, Spain
- ¹⁰ Centro de Investigación y de Estudios Avanzados (CINVESTAV), Mexico City and Mérida, Mexico
- ¹¹ Centro Fermi - Museo Storico della Fisica e Centro Studi e Ricerche "Enrico Fermi", Rome, Italy
- ¹² Chicago State University, Chicago, United States
- ¹³ Commissariat à l'Energie Atomique, IRFU, Saclay, France
- ¹⁴ COMSATS Institute of Information Technology (CIIT), Islamabad, Pakistan

- ¹⁵ Departamento de Física de Partículas and IGFAE, Universidad de Santiago de Compostela, Santiago de Compostela, Spain
- ¹⁶ Department of Physics Aligarh Muslim University, Aligarh, India
- ¹⁷ Department of Physics and Technology, University of Bergen, Bergen, Norway
- ¹⁸ Department of Physics, Ohio State University, Columbus, Ohio, United States
- ¹⁹ Department of Physics, Sejong University, Seoul, South Korea
- ²⁰ Department of Physics, University of Oslo, Oslo, Norway
- ²¹ Dipartimento di Fisica dell'Università and Sezione INFN, Cagliari, Italy
- ²² Dipartimento di Fisica dell'Università and Sezione INFN, Trieste, Italy
- ²³ Dipartimento di Fisica dell'Università and Sezione INFN, Turin, Italy
- ²⁴ Dipartimento di Fisica dell'Università 'La Sapienza' and Sezione INFN, Rome, Italy
- ²⁵ Dipartimento di Fisica e Astronomia dell'Università and Sezione INFN, Bologna, Italy
- ²⁶ Dipartimento di Fisica e Astronomia dell'Università and Sezione INFN, Catania, Italy
- ²⁷ Dipartimento di Fisica e Astronomia dell'Università and Sezione INFN, Padova, Italy
- ²⁸ Dipartimento di Fisica 'E.R. Caianiello' dell'Università and Gruppo Collegato INFN, Salerno, Italy
- ²⁹ Dipartimento di Scienze e Innovazione Tecnologica dell'Università del Piemonte Orientale and Gruppo Collegato INFN, Alessandria, Italy
- ³⁰ Dipartimento Interateneo di Fisica 'M. Merlin' and Sezione INFN, Bari, Italy
- ³¹ Division of Experimental High Energy Physics, University of Lund, Lund, Sweden
- ³² Eberhard Karls Universität Tübingen, Tübingen, Germany
- ³³ European Organization for Nuclear Research (CERN), Geneva, Switzerland
- ³⁴ Faculty of Engineering, Bergen University College, Bergen, Norway
- ³⁵ Faculty of Mathematics, Physics and Informatics, Comenius University, Bratislava, Slovakia
- ³⁶ Faculty of Nuclear Sciences and Physical Engineering, Czech Technical University in Prague, Prague, Czech Republic
- ³⁷ Faculty of Science, P.J. Šafárik University, Košice, Slovakia
- ³⁸ Frankfurt Institute for Advanced Studies, Johann Wolfgang Goethe-Universität Frankfurt, Frankfurt, Germany
- ³⁹ Gangneung-Wonju National University, Gangneung, South Korea
- ⁴⁰ Helsinki Institute of Physics (HIP), Helsinki, Finland
- ⁴¹ Hiroshima University, Hiroshima, Japan
- ⁴² Indian Institute of Technology Bombay (IIT), Mumbai, India
- ⁴³ Indian Institute of Technology Indore, India (IITI)
- ⁴⁴ Institut de Physique Nucléaire d'Orsay (IPNO), Université Paris-Sud, CNRS-IN2P3, Orsay, France
- ⁴⁵ Institut für Informatik, Johann Wolfgang Goethe-Universität Frankfurt, Frankfurt, Germany
- ⁴⁶ Institut für Kernphysik, Johann Wolfgang Goethe-Universität Frankfurt, Frankfurt, Germany
- ⁴⁷ Institut für Kernphysik, Technische Universität Darmstadt, Darmstadt, Germany
- ⁴⁸ Institut für Kernphysik, Westfälische Wilhelms-Universität Münster, Münster, Germany
- ⁴⁹ Institut Pluridisciplinaire Hubert Curien (IPHC), Université de Strasbourg, CNRS-IN2P3, Strasbourg, France
- ⁵⁰ Institute for High Energy Physics, Protvino, Russia
- ⁵¹ Institute for Nuclear Research, Academy of Sciences, Moscow, Russia
- ⁵² Institute for Subatomic Physics of Utrecht University, Utrecht, Netherlands
- ⁵³ Institute for Theoretical and Experimental Physics, Moscow, Russia
- ⁵⁴ Institute of Experimental Physics, Slovak Academy of Sciences, Košice, Slovakia
- ⁵⁵ Institute of Physics, Academy of Sciences of the Czech Republic, Prague, Czech Republic
- ⁵⁶ Institute of Physics, Bhubaneswar, India
- ⁵⁷ Institute of Space Science (ISS), Bucharest, Romania
- ⁵⁸ Instituto de Ciencias Nucleares, Universidad Nacional Autónoma de México, Mexico City, Mexico
- ⁵⁹ Instituto de Física, Universidad Nacional Autónoma de México, Mexico City, Mexico
- ⁶⁰ iThemba LABS, National Research Foundation, Somerset West, South Africa
- ⁶¹ Joint Institute for Nuclear Research (JINR), Dubna, Russia
- ⁶² Korea Institute of Science and Technology Information, Daejeon, South Korea
- ⁶³ KTO Karatay University, Konya, Turkey
- ⁶⁴ Laboratoire de Physique Corpusculaire (LPC), Clermont Université, Université Blaise Pascal, CNRS-IN2P3, Clermont-Ferrand, France

- ⁶⁵ Laboratoire de Physique Subatomique et de Cosmologie (LPSC), Université Joseph Fourier, CNRS-IN2P3, Institut Polytechnique de Grenoble, Grenoble, France
⁶⁶ Laboratori Nazionali di Frascati, INFN, Frascati, Italy
⁶⁷ Laboratori Nazionali di Legnaro, INFN, Legnaro, Italy
⁶⁸ Lawrence Berkeley National Laboratory, Berkeley, California, United States
⁶⁹ Lawrence Livermore National Laboratory, Livermore, California, United States
⁷⁰ Moscow Engineering Physics Institute, Moscow, Russia
⁷¹ National Centre for Nuclear Studies, Warsaw, Poland
⁷² National Institute for Physics and Nuclear Engineering, Bucharest, Romania
⁷³ National Institute of Science Education and Research, Bhubaneswar, India
⁷⁴ Niels Bohr Institute, University of Copenhagen, Copenhagen, Denmark
⁷⁵ Nikhef, National Institute for Subatomic Physics, Amsterdam, Netherlands
⁷⁶ Nuclear Physics Group, STFC Daresbury Laboratory, Daresbury, United Kingdom
⁷⁷ Nuclear Physics Institute, Academy of Sciences of the Czech Republic, Řež u Prahy, Czech Republic
⁷⁸ Oak Ridge National Laboratory, Oak Ridge, Tennessee, United States
⁷⁹ Petersburg Nuclear Physics Institute, Gatchina, Russia
⁸⁰ Physics Department, Creighton University, Omaha, Nebraska, United States
⁸¹ Physics Department, Panjab University, Chandigarh, India
⁸² Physics Department, University of Athens, Athens, Greece
⁸³ Physics Department, University of Cape Town, Cape Town, South Africa
⁸⁴ Physics Department, University of Jammu, Jammu, India
⁸⁵ Physics Department, University of Rajasthan, Jaipur, India
⁸⁶ Physikalisches Institut, Ruprecht-Karls-Universität Heidelberg, Heidelberg, Germany
⁸⁷ Politecnico di Torino, Turin, Italy
⁸⁸ Purdue University, West Lafayette, Indiana, United States
⁸⁹ Pusan National University, Pusan, South Korea
⁹⁰ Research Division and ExtreMe Matter Institute EMMI, GSI Helmholtzzentrum für Schwerionenforschung, Darmstadt, Germany
⁹¹ Rudjer Bošković Institute, Zagreb, Croatia
⁹² Russian Federal Nuclear Center (VNIIEF), Sarov, Russia
⁹³ Russian Research Centre Kurchatov Institute, Moscow, Russia
⁹⁴ Saha Institute of Nuclear Physics, Kolkata, India
⁹⁵ School of Physics and Astronomy, University of Birmingham, Birmingham, United Kingdom
⁹⁶ Sección Física, Departamento de Ciencias, Pontificia Universidad Católica del Perú, Lima, Peru
⁹⁷ Sezione INFN, Bari, Italy
⁹⁸ Sezione INFN, Bologna, Italy
⁹⁹ Sezione INFN, Cagliari, Italy
¹⁰⁰ Sezione INFN, Catania, Italy
¹⁰¹ Sezione INFN, Padova, Italy
¹⁰² Sezione INFN, Rome, Italy
¹⁰³ Sezione INFN, Trieste, Italy
¹⁰⁴ Sezione INFN, Turin, Italy
¹⁰⁵ SUBATECH, Ecole des Mines de Nantes, Université de Nantes, CNRS-IN2P3, Nantes, France
¹⁰⁶ Suranaree University of Technology, Nakhon Ratchasima, Thailand
¹⁰⁷ Technical University of Split FESB, Split, Croatia
¹⁰⁸ The Henryk Niewodniczanski Institute of Nuclear Physics, Polish Academy of Sciences, Cracow, Poland
¹⁰⁹ The University of Texas at Austin, Physics Department, Austin, TX, United States
¹¹⁰ Universidad Autónoma de Sinaloa, Culiacán, Mexico
¹¹¹ Universidade de São Paulo (USP), São Paulo, Brazil
¹¹² Universidade Estadual de Campinas (UNICAMP), Campinas, Brazil
¹¹³ University of Houston, Houston, Texas, United States
¹¹⁴ University of Jyväskylä, Jyväskylä, Finland
¹¹⁵ University of Tennessee, Knoxville, Tennessee, United States
¹¹⁶ University of Tokyo, Tokyo, Japan
¹¹⁷ University of Tsukuba, Tsukuba, Japan
¹¹⁸ Université de Lyon, Université Lyon 1, CNRS/IN2P3, IPN-Lyon, Villeurbanne, France

- ¹¹⁹ V. Fock Institute for Physics, St. Petersburg State University, St. Petersburg, Russia
¹²⁰ Variable Energy Cyclotron Centre, Kolkata, India
¹²¹ Vestfold University College, Tønsberg, Norway
¹²² Warsaw University of Technology, Warsaw, Poland
¹²³ Wayne State University, Detroit, Michigan, United States
¹²⁴ Wigner Research Centre for Physics, Hungarian Academy of Sciences, Budapest, Hungary
¹²⁵ Yale University, New Haven, Connecticut, United States
¹²⁶ Yonsei University, Seoul, South Korea
¹²⁷ Zentrum für Technologietransfer und Telekommunikation (ZTT), Fachhochschule Worms, Worms, Germany